

# Spin Transfer Torque Evaluation Based on Coupled Spin and Charge Transport: A Finite Element Method Approach

**Simone FIORENTINI**

Christian Doppler Laboratory for Nonvolatile Magnetoresistive Memory and Logic  
at the Institute for Microelectronics, TU Wien  
Wien, 1040, Austria

**Johannes ENDER**

Christian Doppler Laboratory for Nonvolatile Magnetoresistive Memory and Logic  
at the Institute for Microelectronics, TU Wien  
Wien, 1040, Austria

**Siegfried SELBERHERR**

Institute for Microelectronics, TU Wien  
Wien, 1040, Austria

**Wolfgang GOES**

Silvaco Europe Ltd, Silvaco Technology Centre Compass Point St Ives  
St Ives, PE27 5JL, United Kingdom

**Viktor SVERDLOV**

Christian Doppler Laboratory for Nonvolatile Magnetoresistive Memory and Logic  
at the Institute for Microelectronics, TU Wien  
Wien, 1040, Austria

## ABSTRACT <sup>1</sup>

Emerging spin transfer torque magnetoresistive random access memories (STT MRAM) are nonvolatile and offer high speed and endurance. MRAM cells include a fixed reference magnetic layer and a free-to-switch ferromagnetic layer (FL), separated by a tunnel barrier. The FL usually consists of several sub-layers separated by nonmagnetic buffer layers. The magnetization dynamics is governed by the Landau-Lifshitz-Gilbert (LLG) equation supplemented with the corresponding torques. To accurately design MRAM cells it is necessary to evaluate the torques in composite magnetic layers, which depend on nonequilibrium spin accumulation generated by an electric current. Spin accumulation and current also depend on the magnetization. Therefore, the LLG and the spin-charge transport equations must be solved simultaneously. We apply the finite element method (FEM) to numerically solve this coupled system of partial differential equations. We follow a modular approach and use well-developed C++ FEM libraries. For the computation of the torques acting in a magnetic tunnel junction (MTJ), a magnetization-dependent resistivity of the tunnel barrier is introduced. A fully three-dimensional solution of the equations is performed to accurately model

the torques acting on the magnetization. The use of a unique set of equations for the whole memory cell is an ultimate advantage of our approach.

**Keywords:** MRAM, Spin Accumulation, Spin Transfer Torque, Spin and Charge Drift-diffusion, Finite Element Method.

## 1. INTRODUCTION

The introduction of a novel nonvolatile memory is essential to mitigate the increase of the leakages and the stand-by power consumption. To be competitive, emerging nonvolatile memories must outperform the traditional CMOS-based memory and flash, by offering superior integration density, fast switching, long retention, high endurance, and low power consumption. At the same time, they must possess a simple structure to reduce fabrication costs and be compatible with CMOS processes to benefit from the advantages provided by the well-developed CMOS fabrication technology.

Previous memory applications driven by magnetic moments and fields played an important role in magnetic

---

<sup>1</sup> All authors of the paper contributed to the proof-reading and copy-editing of the text.

tapes and hard disk drives. An efficient coupling between the electrical and the magnetic degrees of freedom causes a relatively newly discovered phenomenon called giant magnetoresistance effect. Unique properties of magnetic tunnel junctions (MTJs), a sandwich of two ferromagnetic layers (the reference layer (RL) and the free layer (FL)) separated by a tunnel barrier (TB), prompted the introduction of the next generation of memory devices. The tunneling current through the MTJ structure strongly depends on the relative polarization of the ferromagnetic contacts and the tunneling magnetoresistance ratio (TMR) can reach several hundred percent at room temperature [1]. The magnetization of an MTJ can be in two states with distinct relative orientations: parallel and antiparallel. As the resistances in the two states differ by a factor of three, the magnetization state can be used to store the binary information. Memories employing the dependence of the resistance on the relative magnetization orientation are called magnetoresistive random access memories (MRAM). As their MTJ resistances are similar in values to the resistances of MOSFETs, MRAM devices are electrically compatible with CMOS devices.

To write the data in MRAM, the relative magnetization orientation must be changed. The spin-transfer torque effect (STT) [2], [3] has been proven to be particularly useful for a purely electrical magnetic moment manipulation. The torque is generated by a current passing through an MTJ. Electrons' spins become aligned with the ferromagnetic layer magnetization when they travel through the MTJ. In the case of a FL magnetization misaligned with that of the pinned layer, the traveling electrons' spin follows the magnetization and rotates. The change in the spin of the electrons is transferred to the FL magnetization due to the conservation of the angular momentum. As a result, the spin-polarized current exerts a torque on the magnetization of the FL. If the current is sufficiently strong, this torque causes magnetization switching. By inverting the current direction, the sign of the torque and the magnetization switching direction can be inverted.

STT-MRAM is a perfect candidate for future universal memory applications. STT-MRAM is fast (10ns), possesses high endurance (10<sup>12</sup>), and has a simple structure. Several solutions for embedded applications are available: An 8 Mb 1Transistor-1MTJ STT-MRAM on a 28 nm CMOS logic platform [4], a 128 Mb embedded MRAM with 14 ns write speed [5], an embedded MRAM solution compatible with 22FFL FinFET technology [6]. Even though the first commercial STT-MRAM-based products become available, one critical aspect of the currently used STT-MRAM technology, a relatively high switching current, has not been convincingly resolved. The high switching current and large writing energy may jeopardize the advantages provided by nonvolatility, therefore the current needs to be properly optimized. To do so, the torques must be accurately evaluated. We briefly describe our finite element-method (FEM) based

modeling and simulation approach to evaluate coupled three-dimensional charge and spin transport and the corresponding spin-transfer torques driving the magnetization dynamics. The implementation is done by using well supported FEM libraries under open-source licenses.

## 2. SPIN AND CHARGE TRANSPORT EQUATIONS

The spin-transfer torque acting on the magnetization can be modeled by employing Slonczewski's expression of the form [2]

$$\mathbf{T}_S = \gamma \frac{\hbar}{2e} \frac{J_C P_{RL}}{d(1 + P_{FL} P_{RL} \cos \theta)} \mathbf{m} \times (\mathbf{m} \times \mathbf{x}), \quad (1)$$

where  $\hbar$  is the reduced Plank constant,  $e$  is the electron charge,  $J_C$  is the current density,  $d$  is the thickness of the free layer,  $P_{FL}$  and  $P_{RL}$  are the polarizations of the FL and RL, respectively,  $\theta$  is the angle between magnetization vectors in the FL and RL, and  $\mathbf{x}$  is the unit vector along the magnetization direction of the RL. This approach, however, permits to only simulate the dynamics in the thin free layer of a single magnetic tunnel junction (MTJ). A more complete and general description of the switching process is achieved by computing the spin accumulation  $\mathbf{S}$  across the whole structure.

In order to do this, we employ the drift-diffusion formalism. The equations for the spin current, spin accumulation and for the torque acting on the magnetization are

$$\mathbf{J}_S = \frac{\mu_B}{e} \beta_\sigma \left( -\mathbf{J}_C + \beta_D D_e \frac{e}{\mu_B} [(\nabla \mathbf{S}) \mathbf{m}] \right) \otimes \mathbf{m} - D_e \nabla \mathbf{S}, \quad (2a)$$

$$\frac{\partial \mathbf{S}}{\partial t} = -\nabla \mathbf{J}_S - D_e \left( \frac{\mathbf{S}}{\lambda_{sf}^2} + \frac{\mathbf{S} \times \mathbf{m}}{\lambda_j^2} + \frac{\mathbf{m} \times (\mathbf{S} \times \mathbf{m})}{\lambda_\phi^2} \right), \quad (2b)$$

$$\mathbf{T}_S = -\frac{D_e}{\lambda_j^2} \mathbf{m} \times \mathbf{S} - \frac{D_e}{\lambda_\phi^2} \mathbf{m} \times (\mathbf{m} \times \mathbf{S}), \quad (2c)$$

where  $\mu_B$  is the Bohr magneton,  $\beta_\sigma$  and  $\beta_D$  are spin polarization parameters,  $D_e$  is the electron diffusion coefficient,  $\lambda_{sf}$  is the spin-flip length,  $\lambda_j$  is the exchange length, and  $\lambda_\phi$  is the spin dephasing length.

The formalism described by (2) has been successfully applied to metallic spin-valves with a non-magnetic spacer layer [7],[8]. Modern STT-MRAM devices, however, are constituted by a magnetic tunnel junction (MTJ), with a TB between the ferromagnetic layers (FM). The drift-diffusion approach needs to be extended to take into account the TMR effect, and to reproduce the torque expected in MTJs. We showed in [9] that the strong dependence of the tunneling resistance on the relative magnetization vector orientation in the FL and the RL,

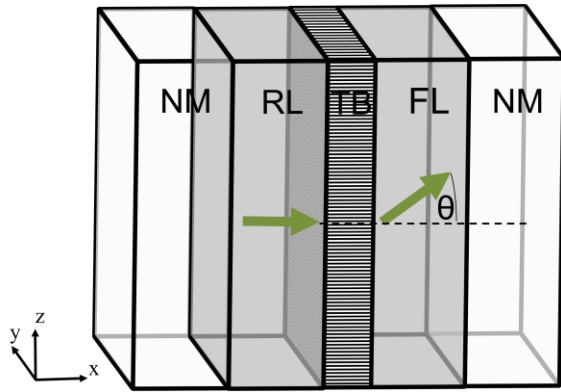


Fig. 1. MTJ structure used in the finite element simulations. The magnetization in the RL is fixed, the one in the FL is free to switch. NM are non-magnetic contact layers.

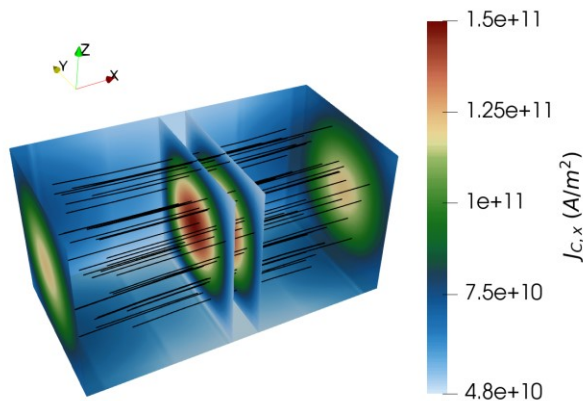


Fig. 2. Current density magnitude obtained for non-uniform magnetization configuration in the FL. The current is highly redistributed at the tunnel barrier interface to accommodate the varying resistance.

described by the TMR ratio, can be reproduced by modeling the TB layer as a poor conductor whose low conductivity incorporates the expected angular dependence. This permits to obtain the electric current  $\mathbf{J}_c$  entering (2a). The current density computed in the structure schematized in Fig.1 for a non-uniform magnetization configuration in the FL, going from parallel in the center to anti-parallel on the sides, is reported in Fig. 2. In the next section, we report the dependence of the average value of the damping-like torque acting on the FL on various system parameters.

The simulations were performed in order to calibrate our approach and reproduce the torque value predicted by

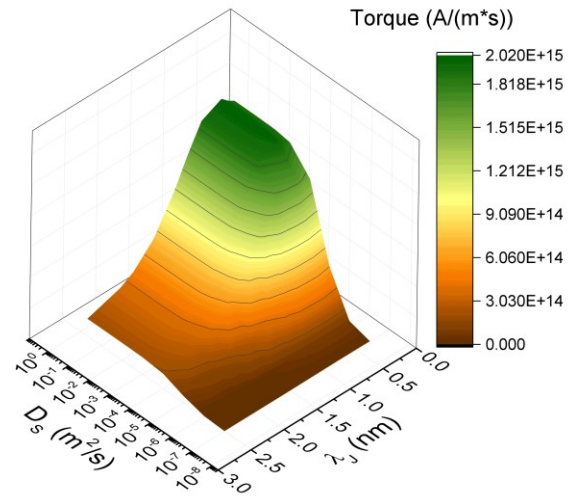


Fig. 3. Dependence of the torque on the exchange length and on the diffusion coefficient of the TB.

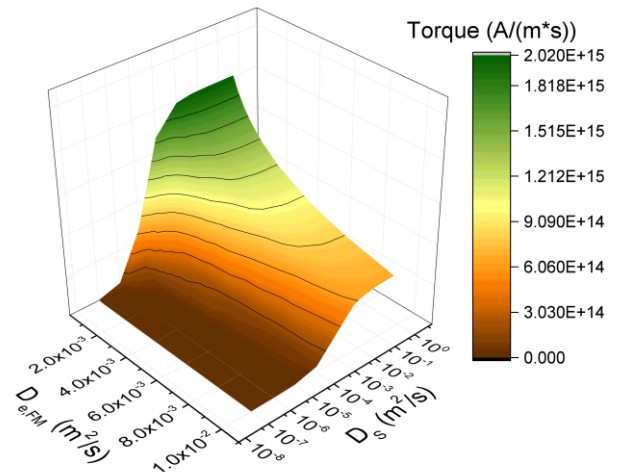


Fig. 4. Dependence of the torque on the diffusion coefficient of the middle layer and on the diffusion coefficient of the FM layers.

Slonczewski in the scope of the drift-diffusion formalism. The spin accumulation is computed via a Finite Element (FE) solver, implemented with the open source library MFEM [10].

### 3. SPIN TRANSFER TORQUE RESULTS

The simulations in this section were carried out in the structure of Fig. 1 with a uniform magnetization, pointing towards the x-axis in the RL and along the z-axis in the FL ( $\theta = 90^\circ$ ). The thickness of the FM layers, the TB and the contacts is 2 nm, 1 nm and 50 nm, respectively.

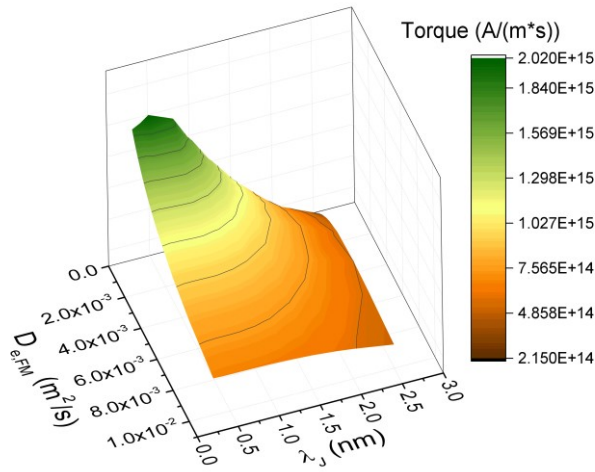


Fig. 5. Dependence of the torque on the exchange length and on the diffusion coefficient of the FM layers.

In Fig. 3 the dependence of the average value of the damping-like torque on the exchange length of the FL and on the diffusion coefficient of the tunnel layer  $D_S$  is reported. In this approach, the equation for the spin accumulation in a tunnel layer with no spin-flips reduces to

$$D_S \nabla^2 \mathbf{S} = 0, \quad (3)$$

and  $D_S$  is a parameter to be chosen properly in order to reproduce the behavior of the torques in an MTJ. Low values of  $D_S$  greatly reduce the torque, while high values enhance the torque, as the slope of all the components of  $\mathbf{S}$  in the middle layer reduces to the point of them being preserved across the barrier. Regardless of the value of  $D_S$ , the torque is enhanced by lower values of  $\lambda_j$ , as they allow the transverse components of the spin accumulation to be completely absorbed in the space of the FL. Fig. 4 reports the dependence on  $D_S$  and on the diffusion coefficient of the FM layers  $D_{e,FM}$ . For high values of  $D_S$  the torque increases as  $D_{e,FM}$  decreases, as a reduction of diffusive effects allows for the transverse spin components to relax faster, while the lower values of  $D_S$  reduce both the torque and its dependence on  $D_{e,FM}$ . In Fig. 5 the dependence on  $D_{e,FM}$  and on  $\lambda_j$  is reported. The interplay between these two parameters is such that a lower diffusion coefficient both increases the average torque and makes it depend more on the value of the exchange length. The torque is maximized by the lower values of both parameters.

We also investigated the dependence on the conductivity polarization parameters  $\beta_{\sigma,FL}$  and  $\beta_{\sigma,RL}$  of the FL and RL, respectively. The results for these simulations are reported in Fig. 6. The average torque value in the FL is mainly dependent on  $\beta_{\sigma,RL}$ , and it is almost unperturbed by variations of  $\beta_{\sigma,FL}$ . These observations suggest that, in our

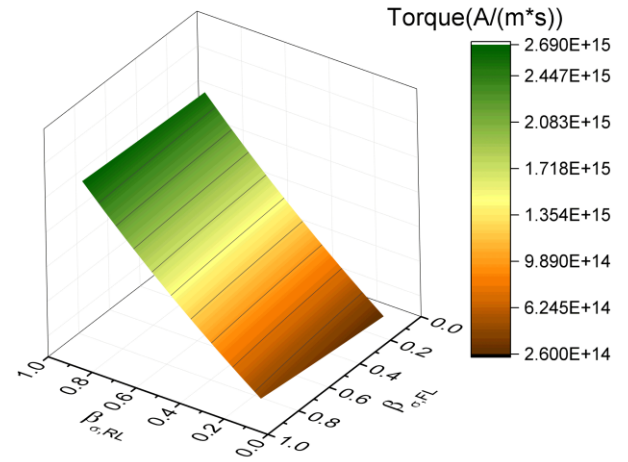


Fig. 6. Dependence of the torque on the polarization of the FL and the RL.

approach,  $\beta_{\sigma,RL}$  and  $\beta_{\sigma,FL}$  are analogous to the polarization parameters  $P_{RL}$  and  $P_{FL}$  entering (1).

With the set of parameters reported in Table 1, the simulation gives an average damping-like torque of  $2.02 \cdot 10^{15}$  A/(m · s), which is compatible with the value  $2.03 \cdot 10^{15}$  A/(m · s) computed using (2). The drift-diffusion approach is thus able to reproduce the torque magnitude expected in magnetic tunnel junctions, with the advantage of being able to compute the torque acting on all the magnetic layers in the structure. In Fig. 7, the spin accumulation and torque computed by the FE solver are compared to an analytical solution, obtained by extending the results from [11] to a multi-layered structure. The comparison shows that the results are in perfect agreement. The FE solver can then be applied to compute the torques for arbitrary magnetization configurations, as exemplified by Fig. 8, where we report the torque magnitude obtained for the same magnetization configuration as the one employed for Fig. 2.

TABLE I. PARAMETERS

Parameter	Value
$\beta_{\sigma}$	0.7
$\beta_D$	0.8
$D_{e,NM}$	$1 \times 10^{-2}$ m <sup>2</sup> /s
$D_{e,FM}$	$1 \times 10^{-4}$ m <sup>2</sup> /s
$D_S$	$5 \times 10^{-1}$ m <sup>2</sup> /s
$\lambda_{sf}$	10 nm
$\lambda_j$	0.5 nm
$\lambda_{\varphi}$	5 nm

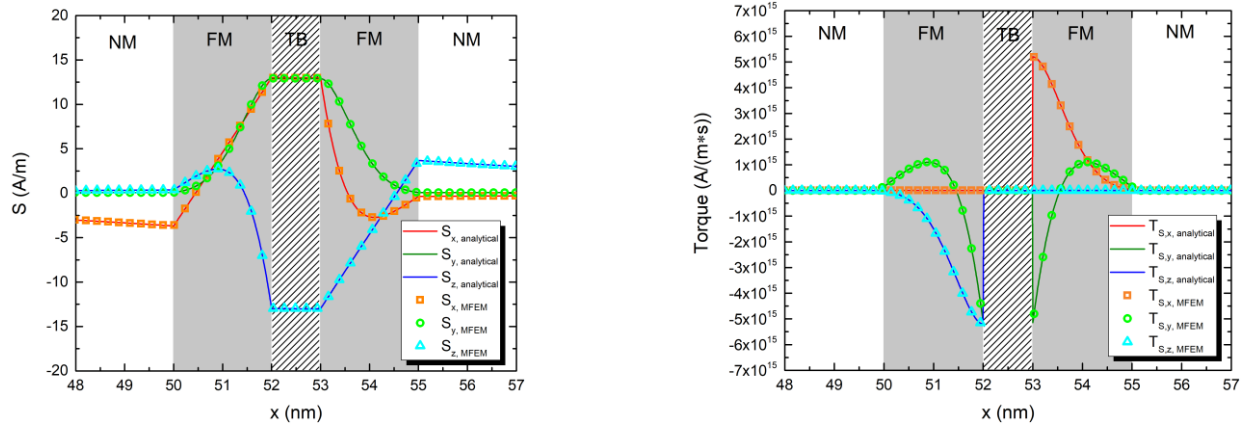


Fig. 7 Comparison of the spin accumulation (left) and torque (right) computed analytically and with the FE solver.

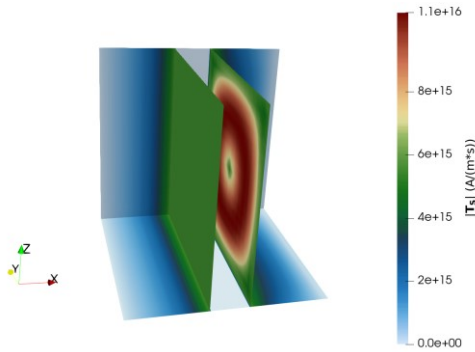


Fig. 8. Spin torque magnitude obtained for the same magnetization configuration as the one employed for Fig. 2. The mesh slices are located at the RL (left) and FL (right) interfaces with the TB.

#### 4. CONCLUSION

A finite element method-based implementation was employed to solve the coupled spin and charge transport equations to evaluate the spin accumulation and the torques acting on a free layer in an MTJ. We investigated the dependence of the spin-transfer torque on system parameters and demonstrated that our approach reproduces the torque magnitude in an MTJ. We compared the finite element results with a known analytical solution which was reproduced by the solver. A complete 3D solution of the coupled spin and charge transport is necessary in order to account for the torque's dependence on the local magnetization. The drift-diffusion solver can now be applied to determine the magnetization dynamics in modern STT-MRAM devices.

#### 5. ACKNOWLEDGMENT

The financial support by the Austrian Federal Ministry for Digital and Economic Affairs, the National Foundation for Research, Technology and Development, and the Christian Doppler Research Association is gratefully acknowledged.

#### 6. REFERENCES

- [1] S. Iwasaki, "Perpendicular Magnetic Recording-Its Development and Realization", **Proceedings of the Japan Academy, Ser. B, Physical and Biological Sciences**, Vol. 85, 2009, pp. 37-54.
- [2] J.C. Slonczewski, "Current-driven Excitation of Magnetic Multilayers", **Journal of Magnetism and Magnetic Materials**, Vol. 159, 1996, pp. L1-L7.
- [3] L. Berger, "Emission of Spin Waves by a Magnetic Multilayer Traversed by a Current", **Physical Review B**, Vol. 54, 1996, pp. 9353-9358.
- [4] Y.J. Song, J.H. Lee, H.C. Shin et al., "Highly Functional and Reliable 8Mb STT-MRAM Embedded in 28nm Logic", **Proceedings of the IEDM**, 2016, pp. 663-666.
- [5] H. Sato, H. Honjo, T. Watanabe et al., "14ns Write Speed 128Mb Density Embedded STT-MRAM with Endurance  $>10^{10}$  and 10yrs Retention @85°C Using Novel Low Damage MTJ Integration Process", **Proceedings of the IEDM**, 2016, pp. 608-611.
- [6] O. Golonzka, J.-G. Alzate, U. Arslan et al., "MRAM as Embedded Non-volatile Memory Solution for 22FFL FinFET Technology", **Proceedings of the IEDM**, 2018, pp. 412-415.
- [7] C. Abert, M. Ruggeri, F. Bruckner et al., "A Three-Dimensional Spin-Diffusion Model for Micromagnetics", **Scientific Reports**, Vol. 5, 2015, p. 14855.
- [8] S. Lepadatu, "Unified Treatment of Spin Torques Using a Coupled Magnetisation Dynamics and Three-dimensional Spin Current Solver", **Scientific Reports**, Vol. 7, 2017, p. 12937.
- [9] S. Fiorentini, J. Ender, M. Mohamedou et al., "Computation of Torques in Magnetic Tunnel Junctions Through Spin and Charge Transport Modeling", **Proceedings of the SISPAD**, 2020, pp. 209-212.
- [10] R. Anderson, J. Andrej, A. Barker et al., "MFEM: A Modular Finite Element Methods Library", **Computers & Mathematics with Applications**, Vol. 81, 2021, pp. 42-74.
- [11] S. Zhang, P. M. Levy and A. Fert, "Mechanisms of Spin-polarized Current-driven Magnetization Switching", **Physical Review Letters**, Vol. 88, 2022, p. 236601.